Journal of Marine Research, 59, 949–975, 2001

The near-surface velocity and potential vorticity structure of the Gulf Stream

by T. Rossby[1] and H.-M. Zhang[1]

ABSTRACT

Using Acoustic Doppler Current Profiler and XBT data between 1992 and 1999 from a container vessel that crosses the Gulf Stream twice weekly near 70W, we examine the near-surface velocity, thermal and vorticity structure of the current. These data come from an ongoing sampling program that has as its overall objective to measure the currents between New York and Bermuda to provide a high-quality database for studies of variability and long-term trends in the region.

These Gulf Stream sections, when averaged in natural or stream coordinates, exhibit a remarkable double-exponential structure. The scale-widths of the lateral shear north and south of the velocity maximum, 20 and 34 km respectively, agree well with estimates of the radius of deformation from simple modal analysis (19 and 34 km, respectively). Significantly, the entire Eulerian mean field of the Gulf Stream and over 80% of the eddy kinetic energy can be accounted for in terms of shift and rotation of this simple double exponential structure. The remainder of this variability can be accounted for rather effectively in terms of a limited number of empirical modes. The first and most energetic mode consists of a 'rocking' mode such that the velocity increases on the concave side of meander extrema. The second EOF mode which measures changes in shear on the anticyclonic side, increases as expected when the stream shifts to the south and vice versa to the north. These two account for nearly half of the remaining variability of the Gulf Stream and adjacent waters (26 and 21%, respectively). These modes notwithstanding, the stiffness of the Gulf Stream is striking.

With the help of concurrent XBTs and historical hydrography, we show that the double-exponential velocity pattern is consistent with a uniformity of potential vorticity between the Gulf Stream and recirculating gyres to either side, but not across the velocity maximum where it undergoes nearly a factor 5 change in ~20 km. The ambient eddy field is sufficiently energetic to maintain the uniformity to either side but much too weak to break down the front. Interestingly, the potential vorticity evinces a slight minimum south of the velocity maximum that appears to be robust.

Unlike other locations along the path of the Gulf Stream, specifically the Pegasus line at 73W and the SYNOP array at 68–69W, the current loses water to the north at this site (with no evident gain or loss to the south). Further, at this location the u-v covariances to both sides of the Gulf Stream suggest a conversion of kinetic energy from the eddy to mean flow. We interpret this as a geometric result of the downstream decrease in meandering approaching the *Oleander* line. It appears that patterns of in- and outflow and energetics can be quite site specific, reflecting, we think, preferred states or patterns of the meandering of the Gulf Stream.

1. Graduate School of Oceanography, University of Rhode Island, Narragansett, Rhode Island, 02882, U.S.A.
email: trossby@uri.edu; hzhang@uri.edu

1. Introduction

Between 1980 and 1983, a program often known as the Pegasus program took bimonthly sections of temperature and velocity across the Gulf Stream at a site ~250 kilometers downstream from Cape Hatteras. The sections were constructed from vertical profiles taken at seven to nine sites with 24-km separation. The program sought to determine, from direct measurements of velocity, the contributions by the Gulf Stream to the mean and annual variations in poleward transport of mass and heat in the North Atlantic (Halkin and Rossby, 1985, hereafter HR; Rago and Rossby, 1987). Somewhat unexpectedly, these repeat sections also revealed a remarkable stiffness or rigidity to the Gulf Stream itself; i.e., the width, shape and magnitude of the velocity field remained comparatively invariant regardless of position of the current or direction of flow (HR). It was also found that about two thirds of the eddy kinetic energy (EKE) obtained from the ensemble of sections disappears after reordering them into stream coordinates. This means that much of the Eulerian EKE observed at a point in the current results from the meandering of this fixed structure, and not from some general mesoscale eddy activity. Others have reported a similar 'stiffness' to the current (Hall, 1986; Johns *et al.,* 1995). Even 1500 km farther downstream east of the New England Seamounts, the Gulf Stream still maintains a well-defined width (Bower and Hogg, 1996; Hendry, 1988).

In more recent years another long-term program to examine the variability of the Gulf Stream on decadal time scales has been in operation. The key element in this program consists of regular and continuous measurements of upper ocean currents from the container vessel *MV Oleander* during its weekly roundtrips between Bermuda and Port Elizabeth, New Jersey. This ongoing program has now been in operation for over eight years. The measurements, made with an Acoustic Doppler Current Profiler (ADCP) operating at 150 kHz in the narrowband mode (Flagg *et al.,* 1998) reach to about 250 m in the Slope Sea north of the Gulf Stream and roughly 150 m in the Sargasso Sea. A remarkable result to emerge from the first four and a half years of operation indicated that the lateral structure of the current was even 'stiffer' than anticipated from the Pegasus program (Rossby and Gottlieb, 1998). Thanks to the high-resolution sampling afforded by the ADCP, we found that the near-surface Gulf Stream can be characterized quite effectively as having a single velocity maximum with an exponentially decaying velocity profile to either side. Since that first report, we have collected close to four more years of even higher quality data. In addition to the velocity data, an expendable bathythermograph (XBT) section is taken once a month from the same vessel. These sections provide valuable information on the thermal structure and thereby a link to the corresponding density field.

In this paper we use all data from Fall 1992 to late 1999 to take a detailed look at the velocity and vorticity fields of the Gulf Stream. We first examine the Gulf Stream and its variability in both Eulerian and natural coordinates. We then test the hypothesis that the observed double exponential velocity structure in stream coordinates results from a uniformity of potential vorticity to either side of, but not across, the velocity maximum. Stommel (1958) had shown how the shoaling pycnocline of the Gulf Stream could be

explained as a consequence of uniform potential vorticity on the Sargasso Sea side of the current. Here we extend Stommel's idea to include the Slope Sea side as well. We also consider whether the hypothesized uniformity of potential vorticity results from a mean inflow or an eddy-driven homogenization process that maintains a uniform PV pool to each side of the current.

2. The data

The *Oleander* has been collecting velocity data since the Fall of 1992. Due to novel technical challenges working on a commercial vessel, the quality and quantity of data available for analysis were limited at first; the principal difficulty being that of electrical noise in the shipboard power system. Considerable editing of the raw data was required. Starting in 1996 after the ship had been in drydock for routine biannual service and inspection, the depth penetration and volume of data increased substantially. There may have been some change in shipboard machinery. At that time we also changed the orientation of the ADCP such that both pairs of beams point diagonally down to the sides of the vessel instead of fore-aft and athwartships. Whatever the reason, we now obtain better data in heavier (but not heavy) weather than in the past, mostly on outbound transits. In heavy weather, bubble entrainment under the vessel all but obliterates the acoustics of the ADCP. For the same reason the data return on inbound transits is less due to the ship's light load factor. With the data now in hand, we seek to examine in greater detail the structural stability of the current, and to identify the corresponding dynamical factors responsible for this. These sections provide an extensive data set with exceptional resolution of the upper ocean velocity field: 8 meters in the vertical and 2.4 km in the horizontal (5 minute averaging at 16 Kt vessel speed). We also have surface temperature from all transits (recorded by the ADCP), and once a month XBTs and surface salinities are collected. The temperature profiles will serve as proxy for density. This is of course a limitation near the surface where the *T*/*S* relationship breaks down.

The ADCP data have been processed and archived using the CODAS software package (Firing, 1991). The velocity accuracy depends very heavily upon how well the ship's motion and heading are known. Since 1995 a differential GPS receiver has corrected for the effects of deliberate degrading of GPS navigation (selective availability; a.k.a. dithering). The differential GPS transmission covers the continental shelf, the Slope Sea and usually the entire Gulf Stream. But even without differential GPS, the effect of dithering is quite limited provided one allows for longer averaging in time, 20 minutes, say (Flagg *et al.,* 1998). Since 1995 we also operate a heading GPS system (3D-GPS) which allows us to correct the gyro compass error directly to a heading accuracy of $\pm 0.1°$. This matters since an error of 1° introduces a 0.14 m s^{-1} error in cross-track velocity at a vessel speed of 16 Kts. In case the 3D-GPS malfunctions, we employ an empirically established statistical correction from recent cruises, but the uncertainties can become significant in heavy weather. Under good operating conditions we think the velocities are accurate at the ± 0.03 m s^{-1} level.

At the beginning of every month a volunteer observer joins the ship for a one-week roundtrip to Bermuda. They take XBTs across the shelf, the Slope Sea and the Gulf Stream on the outbound leg and some additional XBTs in the Sargasso Sea on the return leg. The horizontal resolution of the XBTs varies and depends upon location. In the Gulf Stream, profiles are taken about every 25 km. The shelf and Slope Sea sampling program has been in operation for over 20 years. The once-a-month sampling means that only one out of eight crossings will have XBTs and depending upon the weather, the concurrent ADCP data may or may not be very useful. Thus, the number of sections with simultaneous good XBT and ADCP coverage of the core of the Gulf Stream is significantly less than the total number of sections available for analysis.

3. Eulerian and Stream coordinate mean fields

To set the framework for the following analysis, we show first the mean velocity field at 52 m depth all along the *Oleander* transit (Fig. 1). This and the next figure update the corresponding figures published earlier (Rossby and Gottlieb, 1998). We use all data collected between 1992 and late 1999. The US continental shelf and Bermuda seamount can be seen at opposite ends of the section. The large vectors and variance ellipses indicate the position of the Gulf Stream. The surprisingly sharp decrease in variance away from the mean path of the current suggests that the observed variance results mostly from the current itself and is not part of a generally high background eddy field. An even more organized pattern of flow emerges when the data are plotted in the corresponding stream or natural coordinate system. This is done by aligning all sections according to the velocity maximum and plotting, as a function of normal distance, the component of motion parallel to the velocity maximum. We now find a sharp velocity maximum flanked by rapidly decreasing velocities to either side (Fig. 2). While there is evident scatter, the mean value at the peak, 2.05 m s^{-1}, has a standard deviation of only 0.25 m s^{-1}, a very tight scatter considering that it includes variability on all time scales. Mean values and standard deviations are computed every 10 kilometers. The standard deviations are relatively invariant across the stream at 0.24 m s^{-1} increasing to 0.3 m s^{-1} in regions of strong cyclonic and anticyclonic shear. The mean velocity estimates are used to estimate an exponential fit to either side. In doing this we have not used data within 10 km of the maximum due to the rounding of the peak (we return to this later). We do the fit two ways. First, in order to represent the 'baroclinic structure of the Gulf Stream by itself,' we force the velocity to zero at large $|y|$. An iterative least squares approach yields scale-widths of 20 and 34 km for the northern and southern sides, respectively. The light line in Figure 2 is given by

$$u(y) = 2.61\ \exp(y/20) - 0.56\exp(y/5) \quad (y < 0)$$

$$u(y) = 2.75\ \exp(-y/34) - 0.7\exp(-y/8) \quad (y > 0)$$

where the velocity is in m s^{-1} and the distance, y, is in km, positive to the south. The first terms account for the basic exponential fit to either side while the second terms provide for

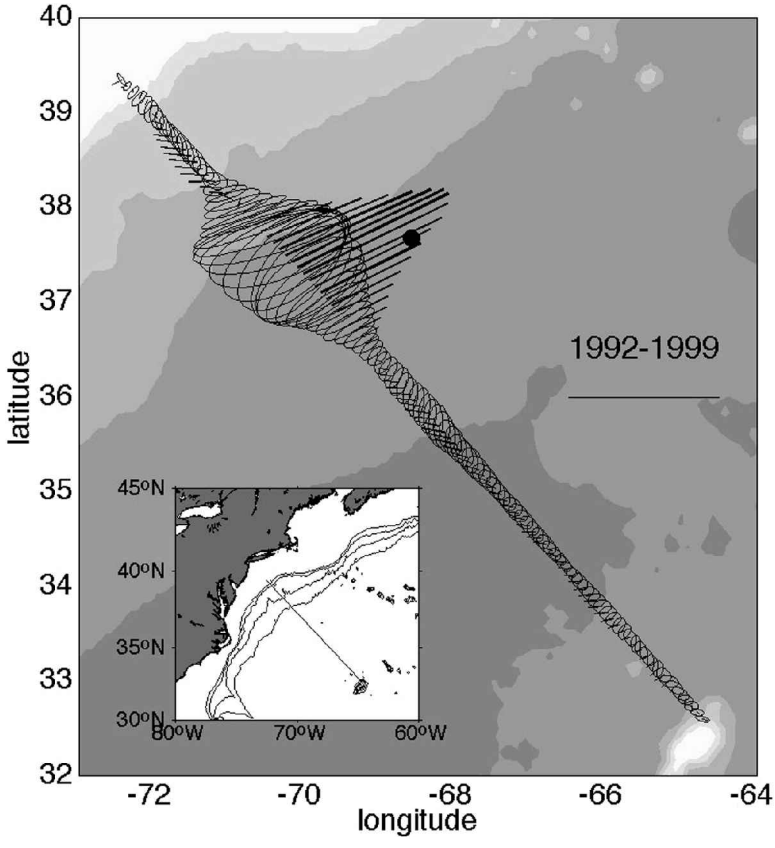

Figure 1. The Eulerian mean field and variance ellipses at 52 m depth from >300 sections across the NW Atlantic. The maximum velocity vector is 500 km from New Jersey. The direction of mean flow is 65°T. The mean flow vectors north of the Gulf Stream suggest a weak outflow, whereas to the south, little exchange appears to be present. Note the very sharp decrease in variance to both sides including a slight minimum. The solid dot indicates the location of the H4 mooring in SYNOP (37° 40′N 68° 35′W). The scale to the right indicates 1 m s^{-1} and 1 J/kg (=m^2 s^{-2}). Bathymetry is indicated in 1000 m increments. The insert shows the location of the *Oleander* line.

the smoothing around the center peak. In the second case we allow the exponential fit to asymptote to the mean flow of the recirculating gyres for large $|y|$. The result, shown by the heavy line in Figure 2, is given by:

$$u(y) = 2.61\ \exp(y/25) - 0.33\ \exp(y/3) - 0.23 \quad (y < 0)$$

$$u(y) = 2.75\ \exp(-y/37) - 0.62\ \exp(-y/3) - 0.08 \quad (y > 0).$$

This set better represents the total velocity field but includes more than the baroclinic Gulf Stream itself, namely a substantially barotropic (i.e., depth-independent) component of -0.23 and -0.08 m s^{-1} in the recirculation gyres north and south of the Gulf Stream,

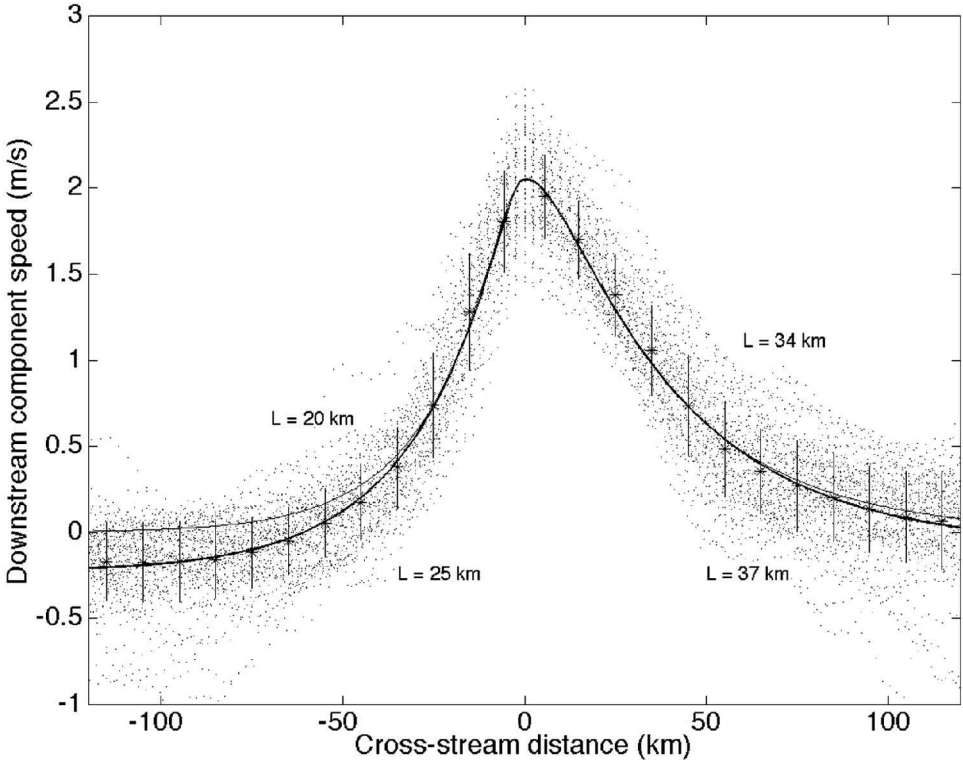

Figure 2. The stream-averaged velocity field of the Gulf Stream at 52 m depth using the same sections as in Figure 1. The dots indicate all velocity components parallel to the maximum velocity vector. The heavy line indicates an exponential fit to these excluding data within 10 km of the maximum (the scale-widths are indicated). The error bars indicate standard deviations in 20 km increments. The light line exponentials are forced to asymptote to zero.

respectively (Hogg, 1992). The difference in scale-widths computed with the two methods is not all that large, an increase from 20 to 25 and 34 to 37 km, respectively. The fit to the round peak, as given by the second set of terms, was done visually.

a. Meandering versus mesoscale eddies

There are two ways one can show that most of the variance in Figure 1 comes from the meandering of the structurally invariant current in Figure 2. In the first approach, we take the observed positions and directions of maximum flow for each and every section and replace all data with data using the analytical form (light line) shown in Figure 2 after projecting them onto the ship's track. The resulting mean field and variance ellipses are shown in Figure 3. The similarity with the observed Eulerian mean fields in Figure 1 is striking. The velocities are almost identical as are the shapes and orientations of the variance ellipses. In the second approach, Figure 4, we compare the eddy statistics for the

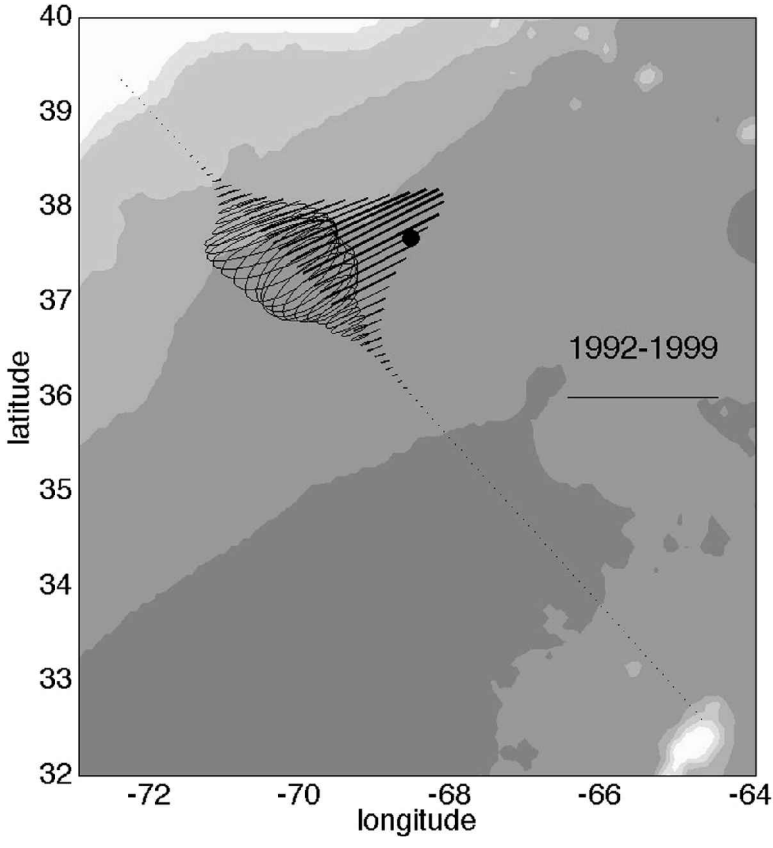

Figure 3. Synthesis of the Eulerian Gulf Stream statistics by mapping the light line in Figure 2 back onto the *Oleander* track. Only the position and direction of the maximum velocity vector are used to orient the double exponential function. Note the striking similarity of both the mean field and variance ellipses with those in Figure 1.

two cases, the original data set (solid line) and the synthetic data set (dashed line) used to prepare Figure 3. We also define a 'residual eddy kinetic energy' (rEKE) by subtracting the analytical representation of the Gulf Stream from the observations (dotted line). First, we note that 80% of the observed EKE in the center of the current can be accounted for by the meandering of a rigid stream. In fact, by adding 0.05 Jkg^{-1} to the dashed line, it coincides almost perfectly with the solid line. But the difference in peak EKE between the observed and synthetic EKE, while comparable, is actually less than the general EKE level to the sides of the Gulf Stream (0.07–0.09 Jkg^{-1}). It is tempting to interpret this as an indication that at this depth the Gulf Stream is acting as a barrier to lateral exchange by submesoscale mixing processes. The rEKE, which measures the departures of the observed velocity field from the double-exponential form, remains nearly invariant across the entire region, but it too evinces a clear

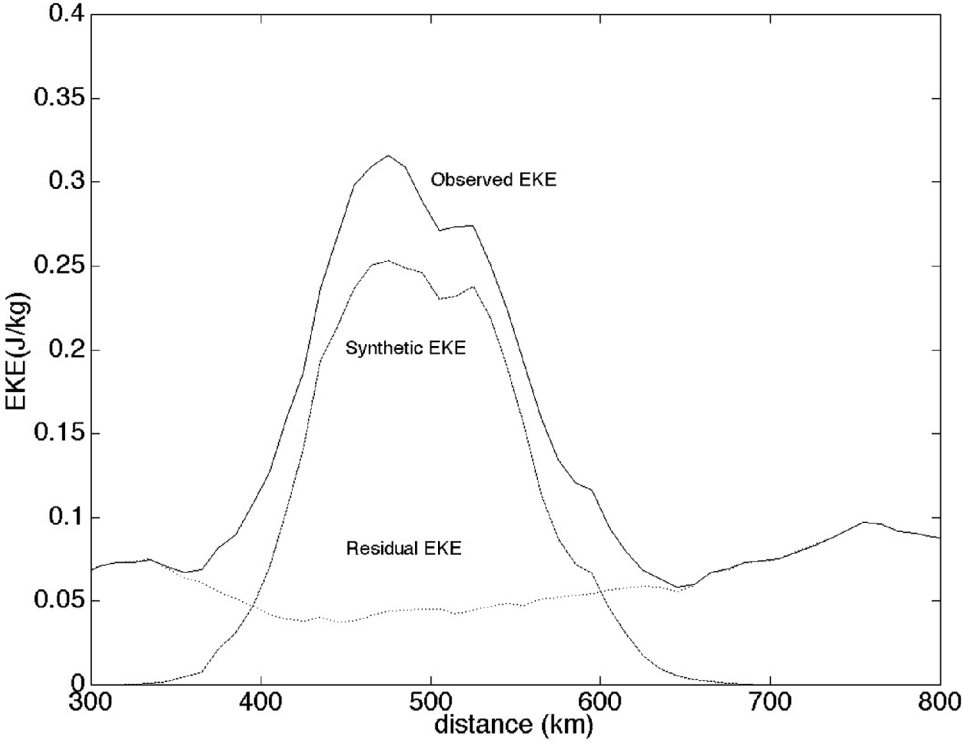

Figure 4. The three curves show the velocity variance in (1) stream coordinates from the observed data, (2) using only the light line double-exponential form in Figure 2, and (3) after first removing the same double exponential function from each transect. The abscissa shows distance in km from New Jersey.

minimum at the center of the current indicating less departure from the 'ideal' form at the center than anywhere else. In summary, here as at the Pegasus line, most of the observed variance in the region of the Gulf Stream stems from the meandering of the current itself, about 67% of the total between 0 and 2000 m at the Pegasus line (HR) and 80% along the *Oleander* line at 52 m depth.

This double-exponential structure is not limited to 52 m, but can be observed at all depths to which the *Oleander* ADCP can reach (the top 150–250 meters, below which the data return drops very rapidly). In Figure 5 we show the downstream velocity on 5 levels, each about 50 meters apart. The peak velocity decreases from 2.05 to 1.74 m s^{-1}. Between the top and bottom levels the maximum velocity shifts south along the *Oleander* line from 491 to 505 km (from the entrance to New York harbor), but without any detectable change in direction. This 14-km shift corresponds to a slope of the velocity maximum of about 1/70 at these depths. The exponential structure remains evident at all levels.

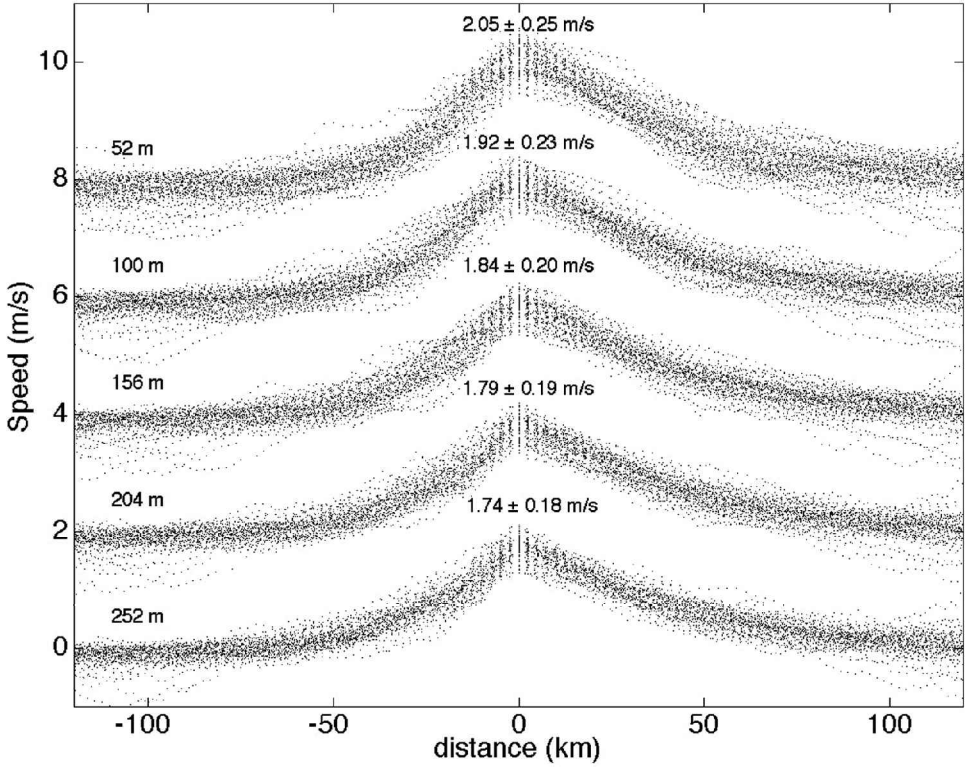

Figure 5. Similar to Figure 2, this shows the stream velocity field in ~50-meter increments from 52 to 252 m depth using 74 high-quality sections for which data at all depths were available. Note the evident exponential structure and cusped velocity peak at all depths. For simplicity, the peak velocities are aligned in the vertical; in reality, the deeper layers are increasingly displaced to the south (see text).

b. Structure of the current

Inspection of individual sections (Fig. 6) reveals considerable variability around the mean structure obtained in the previous section. There is still only one velocity maximum (although small extrema in velocity suggest that embedded submesoscale eddies are not uncommon). The top two panels represent crossings when the stream is far north and south. In the first case we note a strong cyclonic shear and weak anticyclonic shear whereas in the second case the anticyclonic shear is much stronger. The middle two panels show examples where the current is weak and stretched to the north or south. The bottom panels show a rather peaked velocity profile. Some of this variability probably reflects shape changes as the current meanders to the north and south, but embedded submesoscale features advected by the current as well as local interactions with a pre-existing eddy field along the flanks of the current must also play a role. We have found no evidence for the Gulf Stream splitting

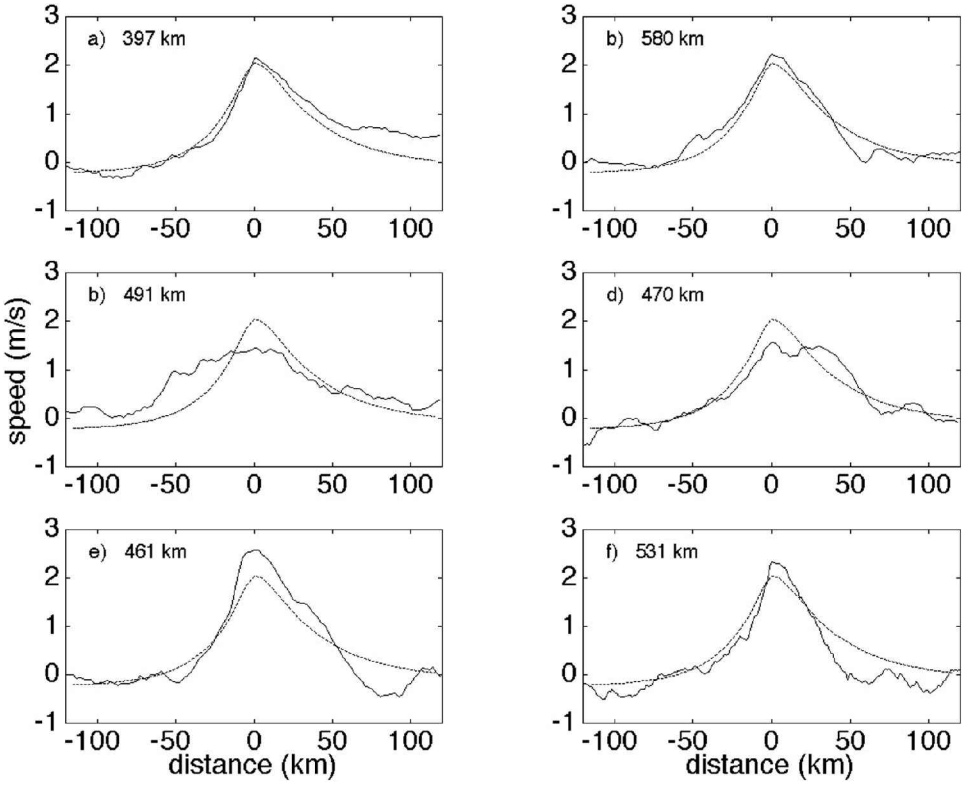

Figure 6. Examples of individual sections across the Gulf Stream with distance of the current axis from New Jersey indicated in the upper left corner. The dotted line shows the double-exponential form. Panels (a) and (b): the current axis is at an extreme northern and southern position, respectively. Panels (c) and (d): weak broad flows. Panels (e) and (f): narrow stronger flows.

into multiple filaments in this area such as has been mentioned in the past (Worthington, 1954).

To gain more insight into the variability of the current structure and to test whether position or direction of flow might have some controlling influence on the shape of the current, we conducted an EOF analysis of the velocity data at 52 m depth. The analysis approach is standard: downstream velocity from the 74 sections in stream coordinates is subsampled at 5 km intervals from −120 to +120 km and the double-exponential structure in Figure 2 (heavy line) is removed so that we only consider the perturbations to the basic structure. A covariance matrix based on the 74 independent sections with 49 equally spaced measurements from each is computed from which the first four eigenmodes and their variances (Fig. 7) are determined. The first two modes account for 47% of the total and the next two for an additional 27%. By projecting each section onto these modes we can obtain a measure of how much each mode contributes to it. Finally, by plotting the

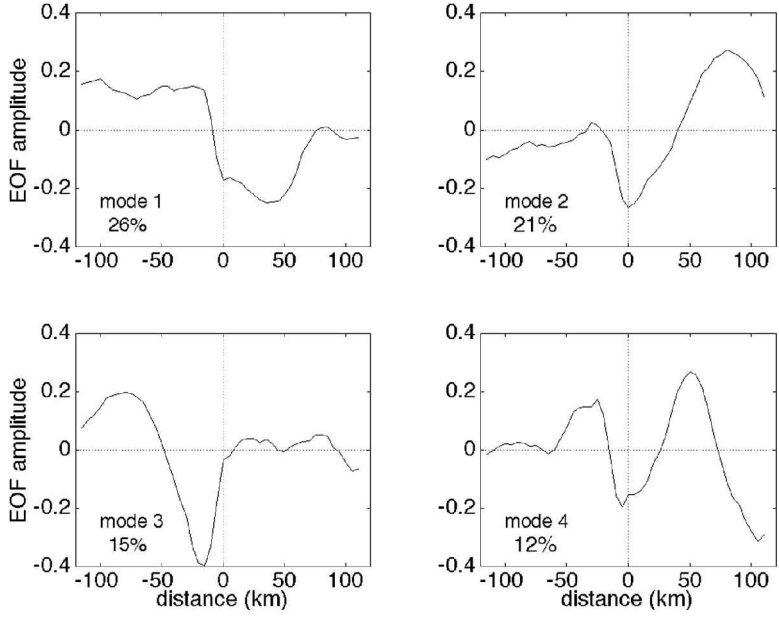

Figure 7. The first four empirical orthogonal (normalized) functions (EOFs) for the velocity field at 52 m depth. The numbers show the % variance accounted for by these modes.

amplitude of the modes against north-south position of the velocity maximum and direction of flow we can check for any correlations between the two. It would be desirable to have curvature information as well, but that is significantly beyond the scope of this study. Instead, we adopt the simplifying assumption that when the stream is meandering to the south it is likely to be curving cyclonically and vice versa when it is in a northerly position. For a simple sine wave along a constant path this should work quite well, but the Gulf Stream is known to undergo gradual shifts north and south on annual and longer time scales (Rossby and Gottlieb, 1998; Rossby and Benway, 2000). Thus, to keep the focus on the meandering, we remove these slow lateral migrations by shifting each observed position by 40*sin ((date − 1993.7)/(6*2π)) km south along the *Oleander* line. This function approximates the gradual southward and northward displacement of the Gulf Stream along the *Oleander* line in the mid- and late 90s as determined from the position of the thermal north wall (see Rossby and Benway, 2000 for further discussion). The resulting scatter plots are shown in Figure 8. We find no connection between the modes and direction of flow, but there does appear to be a correlation between north-south position and the 2nd and 1st modes. Keep in mind that the modes express departures from a mean state, in this case the double-exponential form (heavy line) in Figure 2.

The first mode, upper-left panel in Figure 7, is an antisymmetric mode involving the entire current: when it is positive the flow is stronger on the cyclonic side and weaker on the anticyclonic side. It accounts for 26% of the variance. We might call this a 'rocking

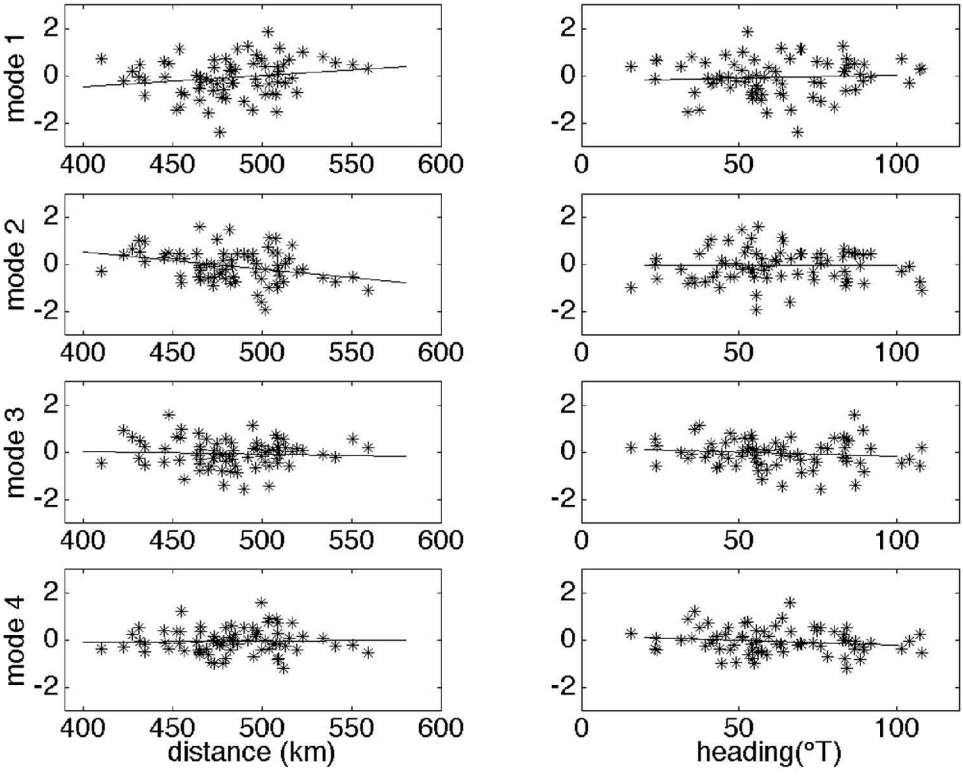

Figure 8. Scatterplots of the amplitudes of the first four modes (top to bottom rows) against north-south position in km from New Jersey (left column) and heading of the Gulf Stream (right column). The lines indicate a linear fit to the data. Only the two first modes show a correlation with north-south position of the Gulf Stream.

mode' because the two sides of the current co-vary but out of phase. The correlation with north-south position is very weak, but indicates that when the stream is in the north, transport weakens on the cyclonic side and increases on the anticyclonic side, and conversely when the stream meanders to the south. To the extent that the correlation is real, it implies that at meander extrema downstream transport by the stream is shifted somewhat toward the concave side of the current; waters on the outside are perhaps more likely to be lost from the current as it passes a crest or trough.

The second mode, upper-right panel in Figure 7, evidently operates between the center and anticyclonic side of the current. When the stream is in a northerly position (Fig. 8, middle left panel), it is positive meaning that the velocity maximum is weaker than average, and stronger when it is displaced to the south. This agrees well with earlier studies (Manning and Watts, 1989; Hummon and Rossby, 1998) which show that the slope of the density surfaces is greater at troughs than at crests. This can be understood as a consequence of the centrifugal force: in troughs it points in the same direction as the

Coriolis force requiring a larger than average pressure gradient near the center of the current where the velocity is greatest. The current achieves this by reducing its width resulting in a greater anticyclonic shear. A linear fit to the data for this case suggests a variation in shear of about 0.07 m s^{-1} per 100 km. The third mode appears similar in shape to the second one, but for the cyclonic side and accounts for 15% of the variance. The fourth mode is roughly symmetric around the velocity maximum and accounts for 12% of the variance. Thus the first four modes account for 74% of the variance.

In summary, while we are not able at this point to identify a strong correlation with external parameters (position, direction), the first mode indicates that the downstream transport is shifted to the concave side of meander extrema, a 'rocking mode,' and the next two modes reflect adjustments due to the curvature of the current, one for the anticyclonic side and the other for the cyclonic side. The fourth and symmetric mode around the velocity maximum might be a varicose mode: when the velocity peaks in the center, it weakens to both sides, meaning the current becomes narrower, and when the center velocity weakens, it increases to both sides and the current widens.

c. Velocity and deformation scales

The scale-widths obtained from the velocity data agree quite well with estimates of the local radius of deformation computed from hydrographic profiles taken just outside the stream to either side (Fig. 9). To see this we use linear theory for planetary wave motion in a stratified ocean. Essentially, we look for the lowest eigenvalue ($i = 1$) for the equation:

$$\frac{d^2w}{dz^2} + \lambda_i^2 N^2 w = 0$$

where N is the Brunt-Väisälä frequency, λ_i are the eigenvalues, and the subscript i refers to mode number. The radius of deformation $= 1/\lambda_i f$ in meters where f = Coriolis parameter $= 0.9 \times 10^{-4}\ s^{-1}$ for this region of the Gulf Stream. Using a set of 30 hydrographic stations near the *Oleander* line just north and south of the Gulf Stream we obtain 19.7 and 34.3 km respectively. These values agree well with estimates made for larger 4° × 4° regions in the vicinity of the Gulf Stream (Emery *et al.,* 1984), and as mentioned above, agree quite well with the scale-widths for the mean velocity shear in Figure 2.

d. Cross-stream velocity

The corresponding normal components of flow follow directly from the transformation from Eulerian to stream coordinates (Fig. 10) (52 m depth only; the others are quite similar). The normal flow components indicate a mean outflow from the stream at this location with a magnitude that reaches about 0.08 m s^{-1} 45 km north of the current axis. The thin lines indicate the standard deviation and the heavy lines the standard error. The latter is based on the number of observations in each bin divided by four (=10 km binwidth/2.4 km sampling rate of the velocity field). The slope of the solid line in Figure 10

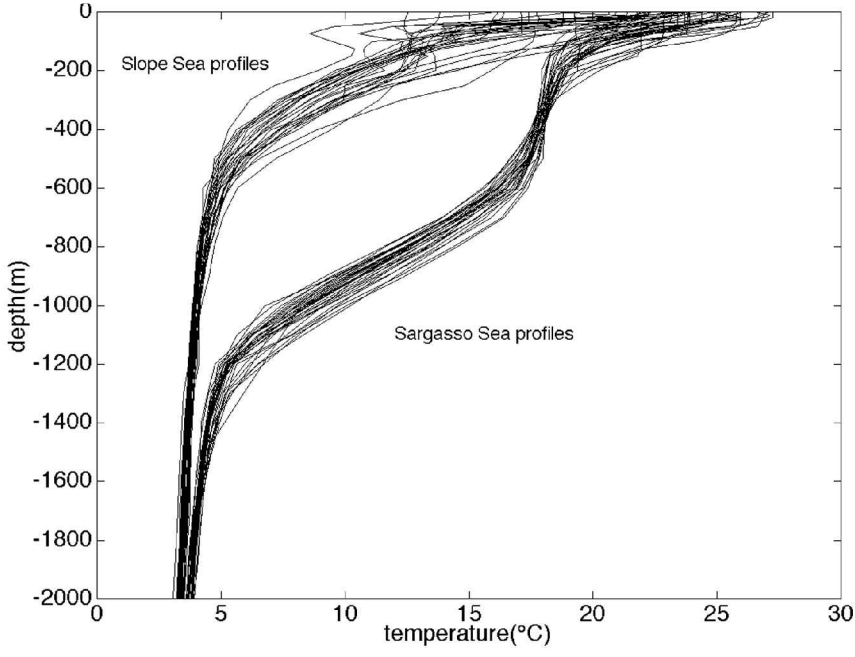

Figure 9. Temperature profiles from 30 hydrographic stations to either side of the Gulf Stream in the immediate vicinity of the *Oleander* line. These and the corresponding salts were used to calculate the radius of deformation (see text).

measures the velocity strain in the plane normal to the stream and equals $1.8 \times 10^{-6}\,s^{-1}$. Loss (or gain) of waters to the south is less clear since the normal velocity component changes sign at various distances from the current axis. A close examination of the mean vectors in Figure 1 shows virtually no exchange with the southern recirculation gyre; the vectors go to zero before turning west.

The outflow to the north contrasts with the HR study in which they note a significant inflow from both sides of the current. The HR program took place just downstream of Cape Hatteras in deepening waters where the meandering envelope shows considerable expansion in the downstream direction. At that site the current is entraining waters from the recirculating gyres both south and north of the Gulf Stream. Our finding also differs from that of Johns *et al.* (1995) who report an inflow from the north in the SYNOP region centered at 68.5W, only 100 km farther downstream. (The central mooring, H4, in their study was centered at the dark dot in Fig. 1.) Figure 6b in their paper is very similar to our Figure 10, but reversed in sign. Thus, the pattern of exchange with the surrounding waters appears to be site-specific and indicates some degree of spatial locking of the current's

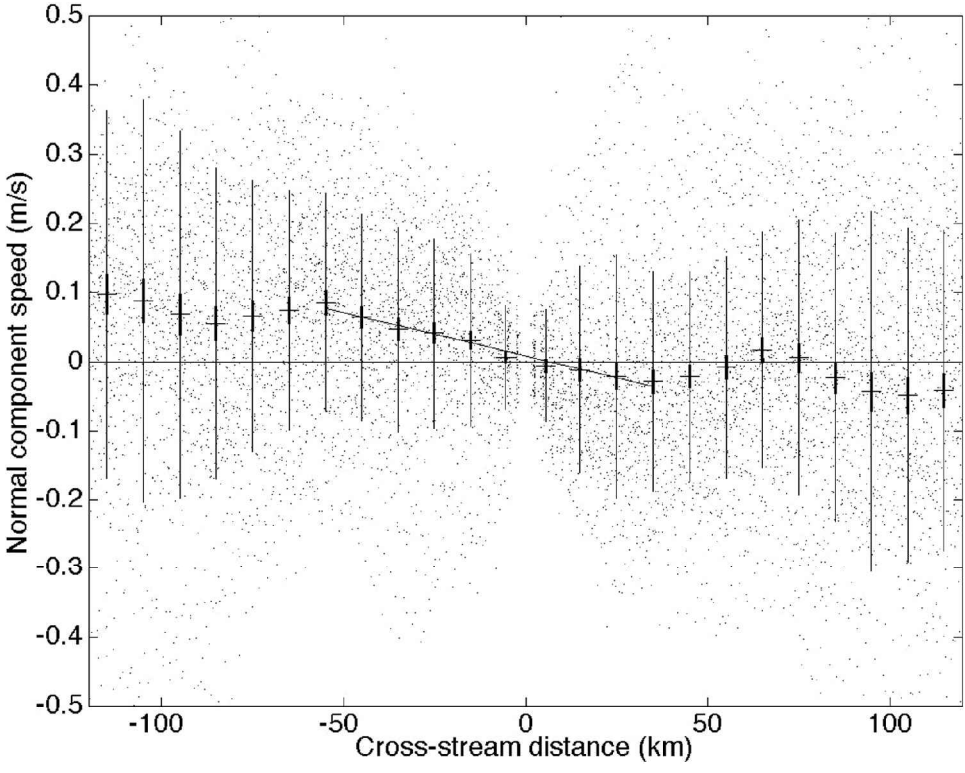

Figure 10. Normal component of flow (relative to the velocity maximum) in stream coordinates (as used for Fig. 2). Note the conspicuous outflow to the north at 0.08 m s^{-1} at −50 km (north of the current axis). The long thin error bars represent standard deviations and the shorter thicker ones standard errors.

meandering. Indeed, the minimum in meander amplitude in this region (the *Oleander* line) suggests the existence of a node of a standing wave (Cornillon, 1986).

Lagrangian studies of the Gulf Stream (Bower and Rossby, 1989; Song *et al.,* 1995) have shown a distinct pattern of entrainment and detrainment in relation to the meandering current. If we knew the path of the Gulf Stream at the time of each *Oleander* transit, we could test the extent to which lateral exchanges correlate with position and curvature of the current. The *Oleander* data cannot give us this information. A useful proxy might be direction of the current such that when the current is pointing north of its ensemble mean direction (65°T), we assume it corresponds to a meander segment between a trough and a downstream crest, and conversely when the vector is pointing south of the mean direction. Figure 11, similar to Figure 10, shows the normal velocity component in stream coordinates as a function of direction relative to the ensemble mean direction (65°T) in 15° direction bins from 30° to −30°. The normal velocity field is clearly difluent around the velocity maximum for positive angles, whereas for negative angles cross-current flow

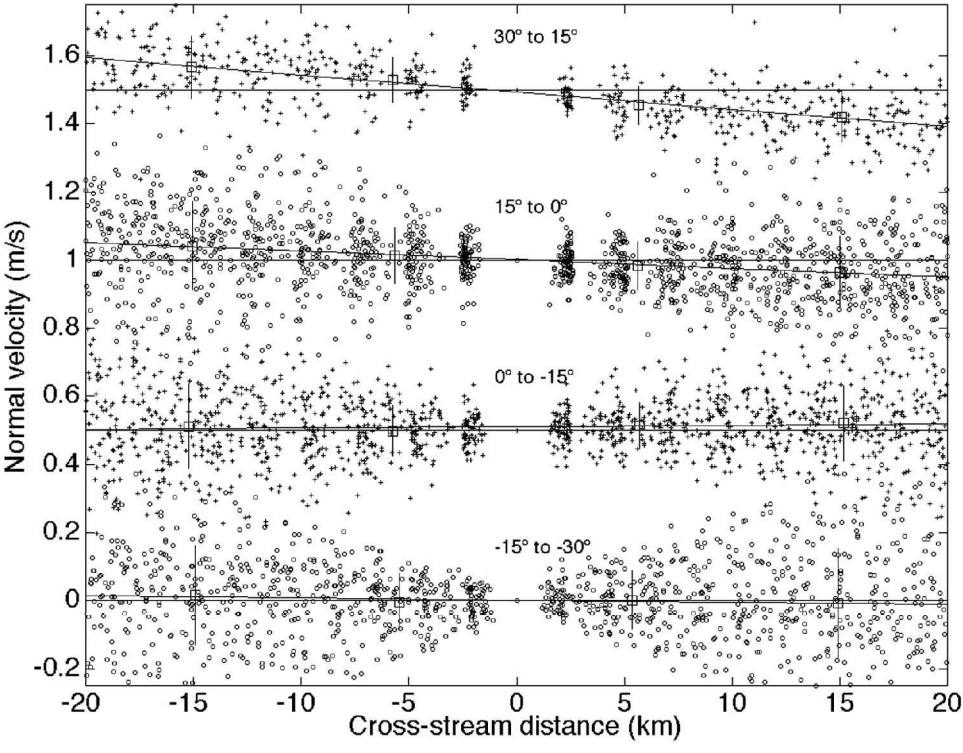

Figure 11. Same as Figure 10 except that the data are grouped into four 15° bins according to direction of the current relative to the 65°T ensemble mean direction of the Gulf Stream. The strongly difluent pattern seen in Figure 7 evidently obtains only when the current has a northerly heading.

shows no gradient and averages close to zero everywhere; i.e., we do not find a reversal, or confluent flow, for large negative or southward directions. This seems to be a robust conclusion given the very large number of sections in each direction group. One possible limitation might be that the ship track with its 135°T orientation intersects the current at such an oblique angle when the current is on a southerly course so as to preclude a proper resolution of the current in this state. We had expected the normal component to exhibit an antisymmetry as the current flows north and south.

e. Thermal structure

As mentioned earlier, XBT sections are taken once per month, thus only a small fraction of the ADCP data have concurrent temperature fields. Further, the XBTs are taken only into the Gulf Stream and not all the way across. This is due to safety concerns for the volunteer observers who at that point have been working for over 24 hours after travelling to the ship from various locations in the country. Still, coverage of the Slope Sea and

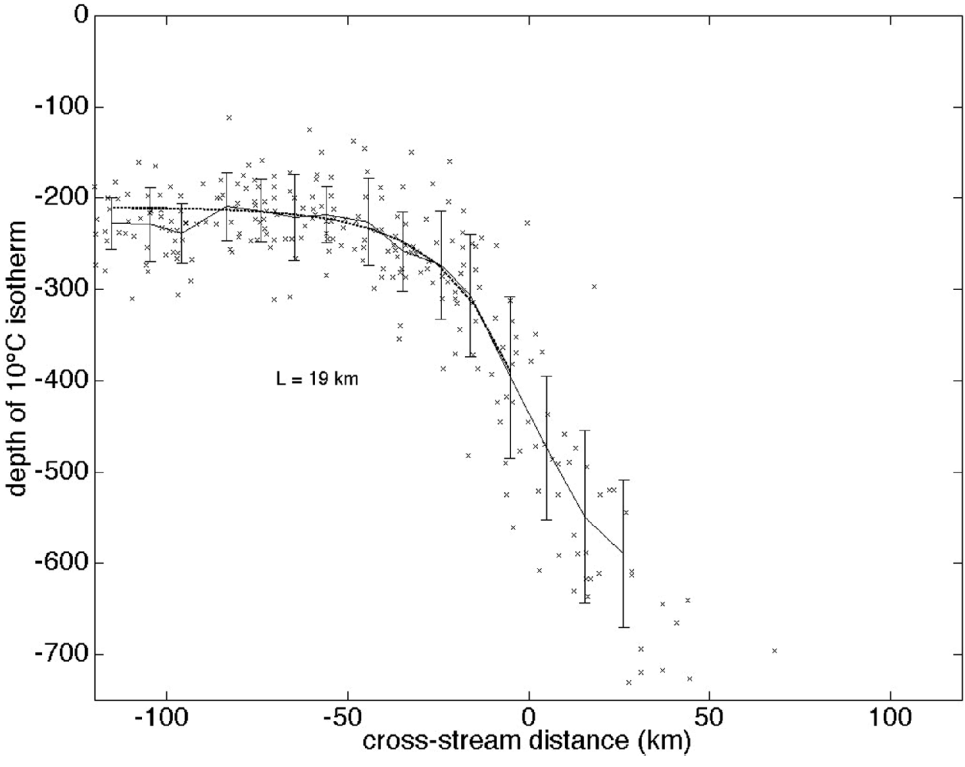

Figure 12. Ensemble-averaged depth of the 10°C isotherm as a function of normal distance from the velocity maximum (as in Fig. 2).

cyclonic side of the Gulf Stream is good. By projecting the XBTs into the same stream coordinate system as used for Figure 2, we can obtain a matching thermal description of the current. The ensemble-averaged depth of the 10°C isotherm is shown in Figure 12. This isotherm lies just below the reach of the seasonal thermocline near the Gulf Stream such that salinity remains invariant in time and essentially constant across the Gulf Stream. It represents the $\sigma_t = 27.2$ surface quite well. The isotherm deepens sharply from north to south across the current. If we fit an exponential to the initial deepening ($y < 0$), we obtain a scale-width of 19 km (dashed line), which agrees reasonably well with the estimates from the velocity field.

4. The mean potential vorticity field in stream coordinates

We now use the stream-averaged estimates of velocity and pycnocline depth to construct the potential vorticity field for the upper layer. We adopt the simplifying assumption that the upper layer moves uniformly, bounded by the $27.0\sigma_t$-surface. We have little choice due to the limited vertical coverage of the velocity field, but we justify this by the observed

fact that the velocity structure of the Gulf Stream can be accounted for extremely well in terms of the barotropic and first baroclinic modes (Rossby, 1987). This means that the upper layer velocity field can be described rather well in terms of a weakly structured vertical shear between the surface and velocity maximum. With regard to choice of interface, we follow Kim and Watts (1994) who found that the $27.0\sigma_t$-surface best approximated the Gulf Stream as a two-layer system in this region (the SYNOP study). Earlier, Rossby (1969) had noted that this (specifically the 12°C) surface best represented the vertical displacements of the thermocline in the Gulf Stream. The relative vorticity is obtained from the lateral shear of the vertically-averaged velocity of the upper layer. While this approach omits the curvature vorticity due to the meandering of the current, very little bias should result since the mean curvature of the current is small. We also include the contribution due to the tilt of the density surfaces. Thus, we write the Ertel (or layer) potential vorticity for the upper layer as:

$$PV = (f + \partial u/\partial n - \partial u/\partial z[(\partial \rho/\partial n)/(\partial \rho/\partial z)])/h$$

where f is the Coriolis parameter, u is the downstream velocity, n is the normal direction to the right looking downstream, z is positive upward, ρ is density, and h is the thickness of the upper layer. The first term represents planetary vorticity, the second term the vertically averaged lateral shear vorticity for the upper layer, and the third term, the contribution from the vertical shear across the sloping layer. The quantity within the square bracket is the slope of an isopycnal, and in this study will be interpreted as the slope of the $27.0\sigma_t$-interface, and is positive on both the cyclonic and anticyclonic sides of the Gulf Stream; i.e., it shoals to the north. As we will see shortly, the third term is quite significant, but only in a very narrow band.

The lateral shear is obtained from a vertical average of the velocities in Figure 5. Since the $27.0\sigma_t$-surface on average lies near 200 m depth on the Slope Sea side, we use the velocities at 52, 100 and 156 m. Between −40 and −20 km we also include the velocities at 204 m and lastly between −20 and +5 km the 252 m depth as well. Actually, these choices are not at all critical to the final result since the PV is controlled far more by the lateral than the vertical shear. South of +5 km on the anticyclonic side we use the vertically averaged velocity of all five layers. This encompasses the 18°C mode water, which has very little vertical shear across it and should represent the warm water pool rather well. The isotachs on this side of the current have a striking vertical orientation due to the almost complete absence of vertical shear (see HR). With respect to pycnocline depth, we use the 30 hydrostations to determine the far-field average depth of the interface, 200 and 830 meters, respectively. We also use the observed 19 km scale-width from Figure 12. For the anticyclonic side a scale-width of 34 km was obtained from the deformation scale analysis above since we have no direct observations (this also ensures that the slope of the interface varies smoothly across the current). The analytical expressions for the vertically integrated velocities and depth are therefore respectively:

$$U(y) = 2.0 \exp(y/26) - 0.51 \exp((y - 5)/7.0) - 0.22 \quad (y < 5)$$

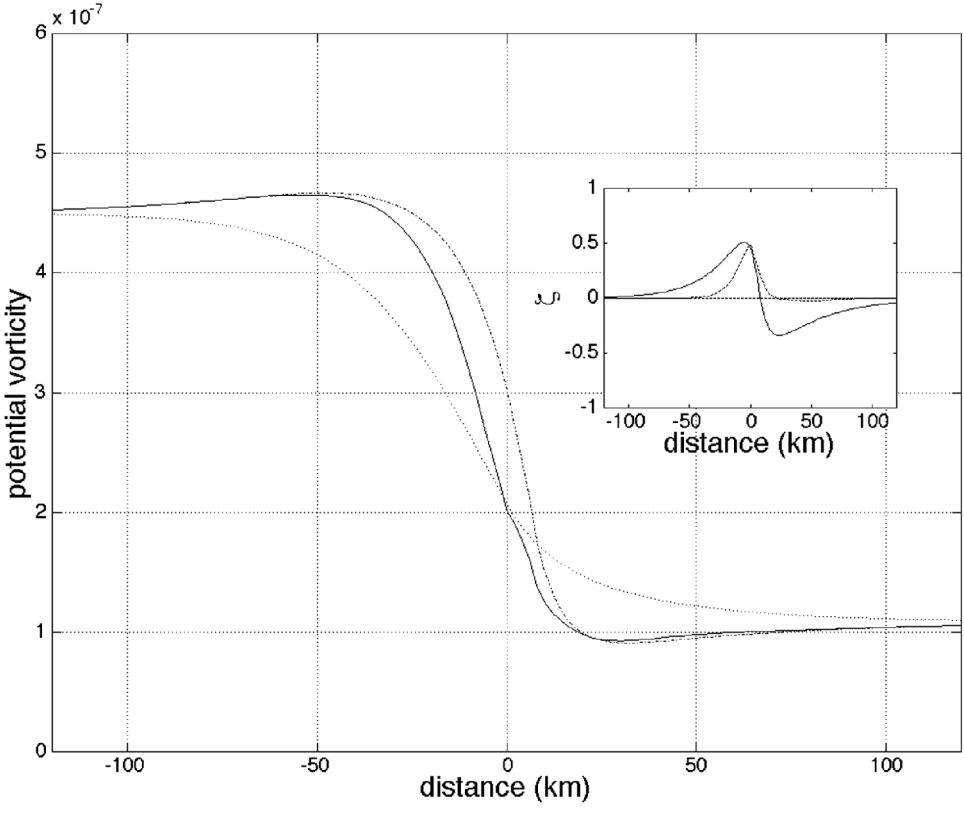

Figure 13. Construct of mean potential vorticity for the upper layer using vertically-averaged velocity very similar to the heavy line in Figure 2 and pycnocline depth in Figure 12. The potential vorticity shows a sharp increase from south to north across the velocity maximum. Note the weak minimum on the anticyclonic side. The insert box shows the normalized (to f) relative vorticity terms used in preparing this figure. See text for further discussion.

$$U(y) = 2.79\ \exp(-y/41) - 0.66\exp(-(y-5)/7.8) - 0.1 \quad (y > 5)$$

and

$$Z_{27.0}(y) = 200 + 235\ \exp(y/19) \quad (y < 0)$$
$$Z_{27.0}(y) = 830 - 395\ \exp(-y/34) \quad (y > 0).$$

Combining these into the expression for potential vorticity (excluding the second relative vorticity term), we obtain the PV distribution plotted as the dash-dot line in Figure 13. As expected, the trends in lateral shear and layer thickness compensate leading to a much sharper transition in PV in the center of the current than any of its constituents. When we include the second relative vorticity term, we obtain the solid line in Figure 13. It has the effect of shifting the entire structure northward about 10 km and with a slight

broadening as well. The dotted line indicates the planetary potential vorticity field alone; i.e., f/h, which varies essentially with the depth of the isopycnal (neglecting all shear terms). The insert shows the ratios of relative vorticity terms to the Coriolis parameter: the first relative vorticity term (solid line) reaches $+0.5$ on the cyclonic side and -0.3 south of the velocity maximum, and the second relative vorticity term (dashed line) is large in a narrow band near the velocity maximum. On the cyclonic side PV remains remarkably uniform (with a slight fractional increase, the significance of which is hard to assess) until it starts to decrease toward the anticyclonic side. However, PV on the southern side shows a minimum in potential vorticity that is about 13% less than its far-field value. At first we assumed it resulted from too strong an anticyclonic shear, possibly due to an overestimate of the vertically averaged velocity from the assumption that the velocities in the warm water pool apply to the entire layer down to the $\sigma_t = 27.0$ surface. But this does not appear to be the case: we used the vertical structure of the velocity field at the Pegasus line to test whether the drop in velocity (vertical shear) across the main thermocline could reduce the vertically averaged velocity enough to remove the minimum. Because of the thickness of the 18°C waters and the weak vertical shear until one gets close to the $\sigma_t = 27.0$ surface, the upper layer velocities apparently do represent the upper layer to within a few centimeters per second. Thus we cannot remove the PV minimum for any realistic variations in scale-width for lateral shear and pycnocline depth and given the far-field limits for $Z_{27.0}$. Watts (1983) has also found a similar PV minimum. In summary, crossing the stream from the Sargasso to the Slope Sea, PV gradually decreases about 13% to a minimum just south of the velocity maximum where it sharply increases almost 5-fold toward the cyclonic side. Whereas the radius of deformation controls the scale-widths of the individual components (depth of upper layer and lateral shear), it does not characterize the PV transition scale, which is much smaller.

5. Eddy exchange processes in the Eulerian frame

Up to now we have emphasized the remarkably stable structure of the Gulf Stream when portrayed in stream coordinates, the double-exponential structure in particular, but also the limited number of modes needed to account for a substantial fraction of the residual variability. This high degree of organization also shows up in the uniformity of the mean potential vorticity field to either side of the maximum stream velocity and provides a clear indication of significant exchange of waters between the Gulf Stream and adjacent waters. In this section we examine the exchange of momentum and heat between the Gulf Stream and the waters to the north where we have a substantial amount of concurrent XBT data. To do this we first need to co-locate all velocity and temperature information, specifically that we identify the velocity profile closest in space to each and every XBT. Since ensemble-averaged profiles are saved every 5 minutes ($\approx$2.4 km), the typical separation between an XBT and the nearest velocity profile is less than 1 km. The correlation between adjacent velocities exceeds 0.95 or more such that the exact separation is of little significance here. There are about 560 co-profiles of velocity and XBTs between the shelf break and the Gulf

Stream. The most important subset (≈48) comprises those within the cyclonic flank of the Gulf Stream where gradients in both velocity and temperature are significant.

We can estimate these covariances in both Eulerian and in stream coordinates. However, since so much of the variance results from the meandering of the relatively rigid structure of the current, the $\langle v'u' \rangle$ correlations in stream coordinates are extremely small, $O(0.03)$. Thus we focus on the Eulerian covariances. The two quantities we estimate will be $\langle v'u' \rangle$ and $\langle v'h' \rangle$ with the primes referring to departures from the corresponding local ensemble mean with u and v representing down- and cross-stream velocity in a framework rotated so that the x-axis and u-velocity point in the mean downstream direction of 62°T. (This differs slightly from the 65°T in Figure 2 due to the smaller data set for which we have both ADCP and XBT data.) The y-direction points to 332°T. The correlation coefficients are about the same, between -0.3 and -0.4 for both momentum and thickness fluxes just north of the Gulf Stream. The minus sign means that the current gains both momentum and thickness from the Slope Sea. Since the along-stream velocity and thickness perturbations u' and h' by themselves are strongly correlated ($= +0.76$, $N = 145$), we interpret the correlation to mean that we are sampling the cross-stream structure of the Gulf Stream at different meander states. The negative correlations mean that the eddy field is converting eddy momentum and thickness back into the mean flow at this site. One way to see this is to consider layer thickness, which decreases monotonically across the Gulf Stream from south to north. A negative correlation $\langle v'h' \rangle$ north of the stream means that when $v' < 0$, $h' > 0$ and thus the meandering is pushing a thick perturbation south toward where h is thicker. The meandering is 'pumping' thickness fluctuations upgradient. Since the stream itself does not change its width, the geometric interpretation becomes that the meanders are decreasing in amplitude as they progress downstream across the *Oleander* line (Cornillon, 1986; Rossby, 1987; Song *et al.,* 1995). Similarly, the orientation of the variance ellipses toward the current from both sides in Figure 1 results from a decreasing meander envelope in the downstream direction forcing the meander-induced eddy field back toward the mean path of the current (Starr, 1968).

A convenient method to get a good measure of the meandering is to examine the trajectories of subsurface floats in the Gulf Stream. Figure 14 shows various paths of the Gulf Stream inferred from the trajectories of 68 isopycnal RAFOS floats drifting on/near the 26.8 sigma-t surface (Song *et al.,* 1995). In preparing this figure, we compute the location where the sloping 15°C ($=26.8\sigma_t$) surface intersects 380 m (close to the velocity maximum on this surface) using the hyperbolic tangent function:

$$y(Z_{15}) = -40 \tanh ((Z_{15} - 380)/300).$$

Given a float's depth, geographical position, direction of motion, we know where it is on this surface and, therefore, can estimate the normal distance to and hence the position of the intersection of 26.8 sigma-t and 380 m depth. Note in Figure 14 the clear convergence of paths as they approach the *Oleander* line and the pattern of sharp spreading farther east; actually, the ship crosses the current virtually where the path crossings have least spread!

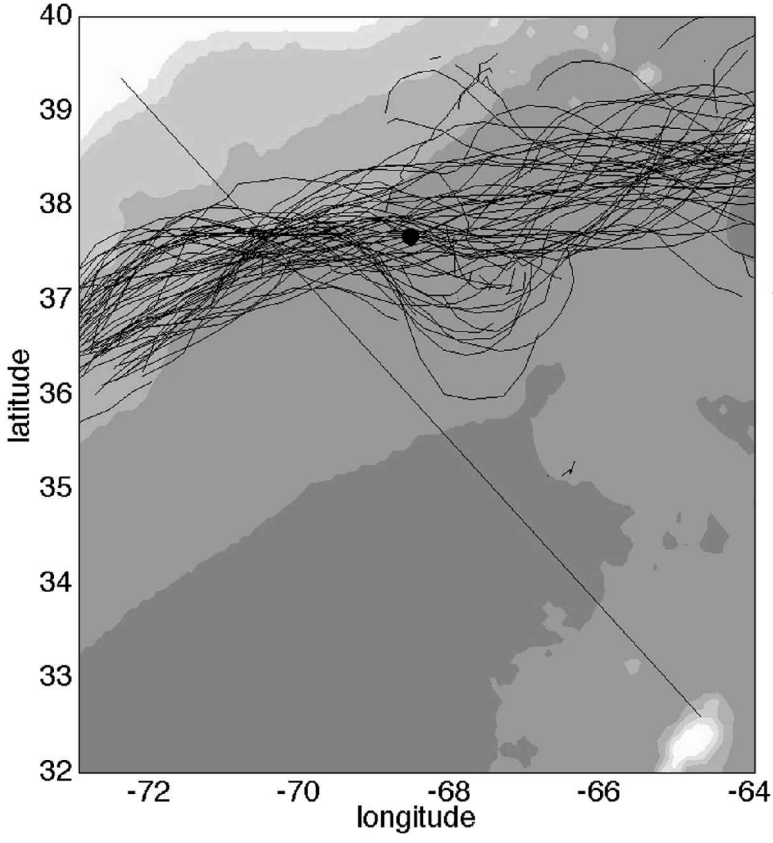

Figure 14. Paths of the Gulf Stream (15°C at 380 m) constructed from 68 isopycnal RAFOS floats on the 26.8σ_t-surface. The line indicates the path of the *Oleander* route.

This convergence of paths reflects the closing of the meander envelope. We think this is the cause of the apparent conversion of momentum and heat back into the mean flow. Just a bit farther to the east, at the black dot, observations show just the opposite, a strong conversion from the mean flow into the eddy field (Johns *et al.,* 1995). Clearly these processes can be quite site-specific.

6. Discussion and summary

This work reaffirms what has become increasingly clear from a number of studies, namely that the Gulf Stream has a very well-defined structure that remains largely invariant as it meanders about. At all locations west of the New England Seamounts every study has found this to be the case. And other studies suggest this remains true farther east as well. Here, thanks to the high resolution sampling, we have been able to probe in further detail the nature of this structural stability. We find that the downstream velocity can be

characterized quite accurately as two back-to-back exponentials with scale-widths quite comparable to the radius of deformation set by the depth of the corresponding pycnocline. This double-exponential structure with an almost discontinuous shear in the center of the current characterizes the velocity field at all sampled depths, 52 to 252 m. This pattern dominates the current so effectively that one can account for 80% of the Eulerian velocity variance in the Gulf Stream region given an invariant velocity structure and where only position and direction of the current varies with time. This result updates earlier studies by Hall (1986) and Johns *et al.* (1995). It seems likely that this stiffness is a general characteristic of other separated western boundary currents such as the Kuroshio Extension (Hall, 1989) and Agulhas Retroflection Current (Lutjeharms and Ansorge, 2001).

The lateral shear on both sides of the current can be understood as a consequence of uniformity of potential vorticity in their respective regions. The increase in shear matches almost perfectly changes in depth of the pycnocline. Stommel (1958) had employed the idea of uniform potential vorticity to explain the shoaling of the Gulf Stream pycnocline. In his case the pycnocline was assumed to surface. Here we assume a symmetry such that uniformity of potential vorticity applies to either side separately but not across the Gulf Stream. As a consequence, potential vorticity undergoes an essentially discontinuous jump across the velocity maximum. Since we have already shown that in this region there is no inflow, we suggest that the eddy activity to either side of the Gulf Stream provides the necessary stirring to maintain the observed uniformity. But this same eddy activity is insufficient to provide mixing across the strong current (Dutkiewicz *et al.,* 2001).

The inability of the eddy activity to extend across the front can be understood kinematically as a consequence of the strong advection by the current itself, which effectively shears apart any local disturbance (Dutkiewicz *et al.,* 1993). Thus the two sides remain isolated from each other. At greater depths (than we can reach here), a weaker downstream advection no longer functions as a barrier to cross-current exchange and the eddy field can instead enhance lateral mixing (Bower *et al.,* 1985; Leaman *et al.,* 1989; Bower and Lozier, 1994).

While the two sides of the Gulf Stream belong to two quite different PV domains, they are both affected by the meandering of the current. The correlation, albeit very weak, between the first mode and north-south position represents, as mentioned, a rocking of the velocity field. When the current curves anticyclonically through crests, the curvature vorticity will decrease everywhere. Since fluid parcels passing through must preserve their PV, they can do so by decreasing layer thickness (stretching vorticity) and/or increasing the shear vorticity. A striking aspect of the first mode is the absence of shear except across the velocity maximum where PV is discontinuous. This absence suggests that, on average, changes in curvature vorticity must be balanced by layer thickness changes. Bower (1989) and Song and Rossby (1997) have shown with their isopycnal float studies that horizontal divergences can, in fact, be quite large. The second mode can be understood more easily in terms of the large variations in anticyclonic shear between meander crests and troughs. In troughs with their strong cyclonic curvature, the shear must turn increasingly anticyclonic

(or the layer must deepen) for a parcel's PV to remain constant. The third mode seems to be the mirror image of the second mode for the cyclonic side of the current. But the variance accounted for by it is only 15% and it shows no correlation with position of the stream.

The transition from one side of the velocity maximum to the other takes place over a scale that is an order of magnitude less than the width of the Gulf Stream itself, about 6 km to either side. This blurring of the velocity maximum, which according to the exponential fit in Figure 2 otherwise would reach 2.7 m s^{-1}, might be described statistically as a consequence of submesoscale mixing. That is to say, in the absence of such mixing the velocity profile would indeed consist of two exponentials that come together into a sharp peak. We can express this loss or blurring of velocity in terms of a submesoscale mixing. One might quantify this using a mixing length argument or in terms of the momentum deficit itself. The traditional mixing length argument says that $K_h \sim \langle v'^2 \rangle^{1/2} l$ where v' represents velocity perturbations normal to the mean flow in stream coordinates and l is the mixing length. We do not have a direct measure of l so we use the mean ($\sim$6 km) of the two scale-widths in the second terms of the equation for mean flow in stream coordinates. This gives us $K_h \approx 1000\ \mathrm{m^2\,s^{-1}}$ ($\sim$900 and $\sim$1100 $\mathrm{m^2\,s^{-1}}$ north and south of the axis, respectively). In the other approach the momentum deficit can be thought of as a balance between the forcing that seeks to establish a purely exponential profile on one hand, and its loss through submesoscale diffusion on the other resulting in the observed velocity profile in Figure 2. We compute the loss as the difference between a purely exponential profile and the one observed in Figure 2, which is given by the second, smaller exponential terms accounting for the rounded peak. This loss takes place through lateral mixing to both sides (hence the factor 2) $\sim 2\langle v'^2 \rangle^{1/2} l = 2K_h$. Integration of the second terms in Section 3 from $-\infty$ to 0 and from 0 to ∞ gives us 8000×0.62 and $4000 \times 0.33 \approx 6280\ \mathrm{m^2\,s^{-1}}$ or $K_h = 3140\ \mathrm{m^2\,s^{-1}}$ as an average for the peak as a whole. This last estimate has the advantage of being an integral estimate. This suggests that the correlation scale, l, may be too small. In summary, the smoothing of the velocity peak can be interpreted as due to a submesoscale diffusivity of about $1\text{–}3 \times 10^3\ \mathrm{m^2\,s^{-1}}$. This can be compared to mesoscale isopycnal diffusivity obtained from the SYNOP float trajectory data which is about an order of magnitude larger at $O(10\text{–}30) \times 10^3\ \mathrm{m^2\,s^{-1}}$ (Zhang *et al.,* 2001).

Unlike the earlier studies of cross-stream flow in the Gulf Stream, the cross-stream flow in this location shows a distinct outflow to the north, and virtually no exchange to the south (in the mean). The HR and Johns *et al.* (1995) studies show clearly an inflow from the Slope Sea, and from the Sargasso Sea as well (HR). The HR study took place just east of Cape Hatteras where the Slope Sea is blocked to the west forcing the west flowing waters to join or attach themselves to the northern edge of the Gulf Stream as it flows east. Similarly, some of the waters in the southern recirculation gyre rejoin the Gulf Stream along its southern flank. Likewise at 68W, Johns *et al.* (1995) report an inflow from the north. Our study, less than 200 km upstream from the Johns *et al.* study, finds the opposite, namely a distinct flow north into the Slope Sea. These differences point to site specific in- and outflows which must, as a consequence, lead to local recirculations embedded in the

general westward drift of the Slope Sea. These are almost certainly related to any standing meander patterns in the Gulf Stream. Rossby (1996) has noted similar features in the North Atlantic Current.

The fact that the eddy kinetic energy (EKE) drops off so sharply outside the envelope of meandering suggests a discreteness or separability of the kinetic energy of the Gulf Stream into two parts, a deterministic kinetic energy due to the meandering of a rigid front and a weak background EKE induced by the meandering. In fact, the residual velocity field has a variance minimum in the center of the current suggesting considerable stability to the jet itself lending further support to the idea that the EKE can be seen as made up of two parts, one due to the superposition of the many different orientations of the (rigid) current itself, and a residual field or perturbation field both inside and outside induced by the meandering. Curiously, the variance ellipses in Figure 1 seem to be smallest just outside the Gulf Stream, beyond which they change only gradually in size across the Slope and Sargasso seas. This minimum in EKE or at least the lack of a gradual decay in EKE away from the Gulf Stream is quite striking. On a related subject, Kim and Rossby (1979) noted a separability of EKE in the Sargasso Sea into a general background field and that due to the presence of cold core rings.

Acknowledgments. This study would not be possible without the help and support of many. Mr. George Schwartze has been responsible for the *Oleander* operations since the start of the project. Dr. Charlie Flagg was instrumental in the design and establishment of the program. Dr. Eric Gottlieb provided crucial support for the first five years of the program. Sandy Fontana provided valuable assistance with the data processing. We thank our colleagues for comments in the course of the preparation of this paper. We are deeply indebted to the Bermuda Container Line and Mr. Cor Teeuwen, in particular, for their continuing support, without which this project would simply not have been possible. Mr. R. L. Benway provided valuable support with the concurrent XBT program and liaison with the Bermuda Container Line. Insightful comments from the reviewers, including the suggestion to assess the last term in the Ertel potential vorticity, are greatly appreciated. The first author would also like to thank Prof. Peter Lundberg at the University of Stockholm, Sweden for his gracious hospitality during a sabbatical visit. Support from NOAA (NA16RC0523 and NA56GP0220), ONR (N000149910064) and NSF (OCE9819724) is gratefully acknowledged.

REFERENCES

Bower, A. S. 1989. Potential vorticity balances and horizontal divergence along particle trajectories in Gulf Stream meanders east of Cape Hatteras. J. Phys. Oceanogr., *19,* 1669–1681.

Bower, A. S. and N. G. Hogg. 1996. Structure of the Gulf Stream and its recirculations at 55°W. J. Phys. Oceanogr., *26,* 1002–1022.

Bower, A. S. and S. M. Lozier. 1994. A closer look at particle exchange in the Gulf Stream. J. Phys. Oceanogr., *24,* 1399–1418.

Bower, A. S. and T. Rossby. 1989. Evidence of cross-frontal exchange processes in the Gulf Stream based on isopycnal RAFOS float data. J. Phys. Oceanogr., *19,* 1177–1190.

Bower, A. S., H. T. Rossby and J. L. Lillibridge. 1985. The Gulf Stream—barrier or blender? J. Phys. Oceanogr., *15,* 24–32.

Cornillon, P. 1986. The effect of the New England Seamounts on Gulf Stream meandering as observed from satellite imagery. J. Phys. Oceanogr., *16,* 386–389.

Dutkiewicz, S., A. A. Griffa and D. B. Olson. 1993. Particle diffusion in a meandering jet. J. Geophys. Res., *98,* 16487–16500.

Dutkiewicz, S., L. Rothstein and T. Rossby. 2001. Pathways of cross-frontal exchange in the North Atlantic Current. J. Geophys. Res., *106* (C11), 26917–26928.

Emery, W. J., W. G. Lee and L. Magaard. 1984. Geographic and seasonal distributions of Brunt-Väisälä frequency and Rossby radii in the North Pacific and North Atlantic. J. Phys. Oceanogr., *14,* 294–317.

Firing, E. 1991. Acoustic doppler current profiling measurements and navigation, *in* WHP Off. Rep. WHP091-1, Scripps Institution of Oceanography, La Jolla, CA, 24 pp.

Flagg, C. N., G. Schwartze, E. Gottlieb and T. Rossby. 1998. Operating an acoustic doppler current profiler aboard a container vessel. J. Atmos. Oceanic Tech., *15* (1, pt. 2), 257–271.

Halkin, D. and T. Rossby. 1985. The structure and transport of the Gulf Stream at 73W. J. Phys. Oceanogr., *15,* 1439–1452.

Hall, M. M. 1986. Assessing the energetics and dynamics of the Gulf Stream at 68W from moored current measurements. J. Mar. Res., *44,* 423–433.

——— 1989. Velocity and transport structure of the Kuroshio Extension at 35N, 152E. J. Geophys. Res., *103* (C10), 14445–14459.

Hendry, R. M. 1988. A simple model of the Gulf Stream thermal structure with applications to the analysis of moored measurements in the presence of mooring motion. J. Atmos. Oceanic Tech., *5,* 328–339.

Hogg, N. G. 1992. On the transport of the Gulf Stream between Cape Hatteras and the Grand Banks. Deep-Sea Res., *39,* 1231–1246.

Hummon, J. and T. Rossby. 1998. Spatial and temporal evolution of a Gulf Stream crest-warm core ring interaction. J. Geophys. Res., *103* (C2), 2795–2809.

Johns, W. E., T. J. Shay, J. M. Bane and D. R. Watts. 1995. Gulf Stream structure, transport and recirculation near 68W. J. Geophys. Res., *100* (C1), 817–838.

Kim, H.-S. and D. R. Watts. 1994. An observational streamfunction in the Gulf Stream. J. Phys. Oceanogr., *24,* 2639–2657.

Kim, K. and T. Rossby. 1979. On the eddy statistics in a ring-rich area: A hypothesis of bimodal structure. J. Mar. Res., *37,* 201–213.

Leaman, K. D., E. Johns and T. Rossby. 1989. The average distribution of volume transport and potential vorticity with temperature at three sections across the Gulf Stream. J. Phys. Oceanogr., *19,* 36–51.

Lutjeharms, J. R. E. and I. Ansorge. 2001. The Agulhas Return Current. J. Mar. Syst., *30,* 115–138.

Manning, J. P. and D. R. Watts. 1989. Temperature and velocity structure of the Gulf Stream northeast of Cape Hatteras: modes of variability. J. Geophys. Res., *94,* 4879–4890.

Rago, T. A. and H. T. Rossby. 1987. Heat transport into the North Atlantic Ocean north of 32N latitude. J. Phys. Oceanogr., *17,* 854–871.

Rossby, H. T. 1969. On monitoring depth variations of the main thermocline acoustically. J. Geophys. Res., *74,* 5542–5546.

——— 1987. On the energetics of the Gulf Stream at 73W. J. Mar. Res., *45,* 59–82.

——— 1996. The North Atlantic Current and surrounding waters: At the crossroads. Rev. Geophys., *34,* 463–481.

Rossby, T. and R. L. Benway. 2000. Slow variations in mean path of the Gulf Stream east of Cape Hatteras. Geophys. Res. Lett., *27,* 117–120.

Rossby, T. and E. Gottlieb. 1998. The Oleander Project: Monitoring the variability of the Gulf Stream and adjacent waters between New Jersey and Bermuda. Bull. Amer. Meteor. Soc., *79,* 5–18.

Song, T. and T. Rossby. 1997. Analysis of Lagrangian potential vorticity balance and lateral displacement of water parcels in Gulf Stream meanders. J. Phys. Oceanogr., *27,* 325–339.

Song, T., T. Rossby and E. Carter. 1995. Lagrangian studies of fluid exchange between the Gulf Stream and surrounding waters. J. Phys. Oceanogr., *25,* 46–63.

Starr, V. 1968. Physics of Negative Viscosity Phenomena, McGraw-Hill Book Company, NY, 256 pp.

Stommel, H. 1958. The Gulf Stream, University of California Press, Berkeley, CA, 202 pp.

Watts, D. R. 1983. Gulf Stream, *in* Eddies in Marine Science, A. R. Robinson, ed., Springer-Verlag, NY, 114–144.

Worthington, I. W. 1954. Three detailed cross-sections of the Gulf Stream. Tellus, *6,* 116–123.

Zhang, H.-M., M. D. Prater and T. Rossby. 2001. Isopycnal Lagrangian statistics from the North Atlantic Current RAFOS float observations. J. Geophys. Res., *106,* 13,817–13,836.

Received: *8 February, 2001;* revised: *28 August, 2001.*